HHS Public Access

Author manuscript

Atherosclerosis. Author manuscript; available in PMC 2021 November 01.

Published in final edited form as:

Atherosclerosis. 2020 November ; 313: 43–49. doi:10.1016/j.atherosclerosis.2020.09.012.

Iodine-enhanced micro-computed tomography of atherosclerotic plaque morphology complements conventional histology

Trevor S. Self[a], **Anne-Marie Ginn-Hedman**[b], **Courtney N. Kaulfus**[c], **Annie E. Newell-Fugate**[a], **Brad R. Weeks**[c], **Cristine L. Heaps**[a,d,*]

[a]Veterinary Physiology and Pharmacology; Texas A&M University, College Station, TX, USA

[b]Biomedical Engineering; Texas A&M University, College Station, TX, USA

[c]Veterinary Pathobiology; Texas A&M University, College Station, TX, USA

[d]Michael E. DeBakey Institute for Comparative Cardiovascular Science and Biomedical Devices; Texas A&M University, College Station, TX, USA

Abstract

Background and aims: Visualization of arterial lesions *in situ* can enhance understanding of atherosclerosis progression and potentially improve experimental therapies. Conventional histology methods for assessing atherosclerotic lesions are robust but are destructive and may prevent further tissue analysis. The objective of the current study was to evaluate a novel, nondestructive method for visualization and characterization of atherosclerotic lesions as an alternative or complementary to routine histology. Thus, we tested the hypothesis that micro-computed tomography (micro-CT) paired with an iodine-based radiopaque stain would effectively characterize atherosclerotic plaques in a manner comparable to routine histology while maintaining sample integrity and providing whole-volume data.

Methods: We examined porcine coronary arteries with varying degrees of atherosclerosis, using micro-CT in the absence and presence of iohexol (240 mgI/ml). Following iohexol washout, routine histological assessment of the samples was performed with hematoxylin and eosin and Masson's trichrome.

*Corresponding author: Cristine Heaps, Department of Veterinary Physiology and Pharmacology, College of Veterinary Medicine and Biomedical Sciences, Texas A&M university, 4466 TAMU College Station, TX 77843-4466. cheaps@cvm.tamu.edu.

Author contributions

Conceptualization: Bradly R. Weeks, Anne-Marie Ginn-Hedman, Cristine L. Heaps, Trevor S. Self. Data acquisition: Anne-Marie Ginn-Hedman, Courtney N. Kaulfus, Trevor S. Self. Methodology: Bradly R. Weeks, Anne-Marie Ginn-Hedman, Courtney N. Kaulfus, Cristine L. Heaps, Trevor S. Self. Writing-original draft: Trevor S. Self. Writing-review and editing: Bradly R. Weeks, Anne-Marie Ginn-Hedman, Cristine L. Heaps, Annie E. Newell-Fugate, Courtney N. Kaulfus Trevor S. Self

Conflict of interest

The authors declared they do not have anything to disclose regarding conflict of interest with respect to this manuscript.

Declaration of interests

The authors declare that they have no known competing financial interests or personal relationships that could have appeared to influence the work reported in this paper.

Results: Iohexol staining generated soft tissue delineation and subsequent atherosclerotic plaque assessment via augmented radiopacity, permitting three-dimensional (3D) reconstruction of these lesions, maintaining *in situ* architecture. Although plaque distribution and arterial wall tissue layers were discernable, micro-CT was incapable of discriminating cell types comprising the plaque. Calcium phosphate deposition was readily located and visualized in 3D space, independent of iohexol.

Conclusions: The results of this study establish micro-CT, combined with a diffusible radiopaque contrast agent, as a powerful imaging modality for visualizing *in situ* architecture of atherosclerotic plaques. Our findings demonstrate that micro-CT can be used to identify plaque distribution and calcium deposition complementary to routine histological analysis.

Graphical Abstract

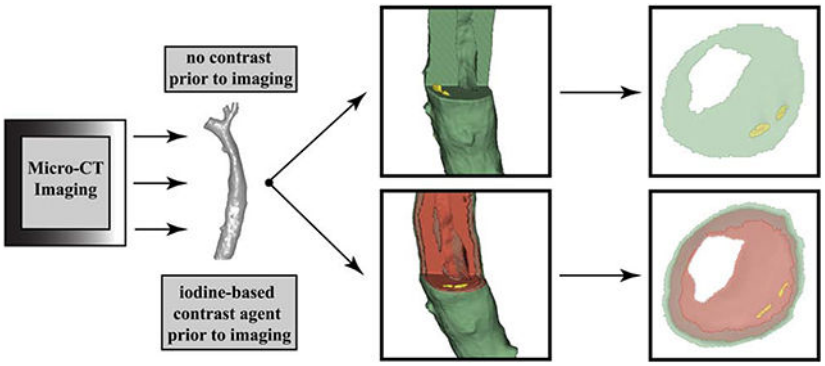

Keywords

cardiac; vasculature; 3D imaging; contrast agent; virtual histology

Introduction

Despite technological advances in methods used to investigate atherosclerotic plaque development and adaptations in response to therapeutic interventions, conventional light microscopy of tissue sections remains the gold standard for studying lesions on the microscopic scale [1]. However, histologic examination is often labor intensive, destructive, and unable to provide full-volume, three-dimensional (3D) morphology of the vascular sample. Furthermore, paraffin or plastic embedding followed by tissue sectioning prevents alternative specimen assessment. While most histologic analyses are based on two-dimensional evaluation (2D), there are histology-based methods for 3D imaging. However, 3D imaging from histology is laborious, limited, and requires specific expertise [2–5].

Micro-computed tomography (micro-CT) is an established imaging technique allowing for nondestructive assessment of tissue with excellent 3D spatial resolution for explanted specimens [6,7]. Micro-CT image acquisition from biological specimens relies on the differences in photon attenuation in various tissue types, with greater photon energy loss across denser tissue such as mineralized bone or implanted metal [8–10]. The primary limitation of micro-CT for imaging soft tissue is the low inherent contrast of nonmineralized

tissues. Therefore, a diffusible radiopaque contrast agent is often required to delineate adjacent soft tissues for micro-CT analysis [11–17].

Commonly used contrast agents often incorporate heavy metals and are expensive, toxic, and require extended staining times [8]. Many of these agents are also irreversible or require ethanol immersion leading to excessive tissue shrinkage [8, 18]. Alternatively, aqueous iodine-based contrast agents, such as Lugol's solution, have been adapted for use in micro-CT imaging as first described by Metscher [12, 19]. Lugol's solution is a radiopaque contrast agent consisting primarily of inorganic iodine in the form of iodine potassium iodide (I_2KI). Lugol's solution exhibits a preferential accumulation in glycogen- or lipid-rich tissues [19–21]. However, the use of Lugol's solution is often limited to anatomical studies due to the need for high concentrations and long staining times [14, 22]

Iodine-based, nonionic, monomer radiopaque contrast agents, such as iohexol (GE Omnipaque 350) and iodixanol (GE Visipaque 320) overcome the limitations of other agents by offering short staining times and water-soluble distribution in tissue. These solutions are used clinically and in research settings as perfusable contrast agents for noninvasive angiography [23], vascular imaging [24], and clinical measurements of glomerular filtration rate and renal clearance [25]. In addition, these solutions are also used as diffusible contrast agents in explanted tissues, though their efficacy in assessing atherosclerotic plaque morphology is not widely described.

Our rationale for these studies was that the maintenance of *in situ* architecture during 3D imaging of atherosclerotic plaques in animal models of coronary artery disease is important for accurate analysis of lesions and evaluation of the effectiveness of potential therapies aimed at altering plaque size, composition, or vulnerability. Thus, we tested the hypothesis that micro-CT paired with the diffusible radiopaque stain, iohexol, could be used to image atherosclerotic plaques in explanted arterial specimens from swine, generating full-volume data while preserving *in situ* architecture of plaques. We further hypothesized that subsequent routine histology could be performed successfully on the same tissue without histological artifact from prior micro-CT with iohexol contrast enhancement.

Materials and methods

Animals.

Ossabaw swine were obtained from the Comparative Medicine Program of Indiana University School of Medicine and Purdue University (West Lafayette, IN). Groups were fed a lean diet (approximately 2000 kcal/pig/day) or an atherogenic diet (approximately 4570 kcal/pig/day) with coconut oil and hydrogenated soybean oil as the primary sources of fat as previously described [26]. All experimental procedures were approved by and performed in compliance with Texas A&M University Institutional Animal Care and Use Committee regulations and followed the guidelines of the Guide for the Care and Use of Laboratory Animals.

Isolation of coronary arteries.

Upon termination, hearts were removed from Ossabaw swine fed lean or atherogenic diets, and coronary arteries were dissected free from surrounding tissue using a stereo microscope. Throughout dissection, tissues were maintained in ice-cold Krebs bicarbonate buffer (0-4 °C) and then isolated arteries were placed in 10% neutral-buffered formalin (NBF) for fixation pending further analysis.

Micro-computed tomography.

A mounting apparatus was designed to suspend and stabilize the samples in air for the duration (approximately 50 min) of the micro-CT image acquisition as illustrated in Figure 1 of the supplementary materials. The vessel ends were pinned to silicon blocks (Sylgard 184, silicon elastomer) using stainless steel pins; the blocks were further pinned to a silicon base prepared axially along one side of a 50 mL polypropylene centrifuge tube. The bottom of the tube was inserted into a polystyrene foam stand for stabilization during imaging.

Coronary arteries were mounted and imaged using a North Star Imaging (NSI) X50 micro-CT machine (Rogers, Minnesota) achieving a spatial resolution of 21.39 μm. The micro-CT geometry and settings are presented in Table 1 of the supplementary materials. Coronary arteries were first imaged using micro-CT without a radiopaque contrast agent as a control. Artery samples were removed from 10% NBF and the lumen cleared of solution via absorption by placing the vessel ends against non-woven surgical gauze. Subsequently, the sample was mounted as described above for micro-CT imaging. Following micro-CT image acquisition, the sample was removed from the mounting apparatus and placed back into 10% NBF.

Diffusible iodine contrast imaging.

In order to generate soft tissue delineation and enhance atherosclerotic plaque visualization, micro-CT imaging was next performed with the water-soluble, iodine-based, diffusible radiopaque contrast agent, iohexol (Omnipaque; 240 mgI/mL; GE Healthcare). Coronary artery segments were removed from 10% NBF and a syringe with an intravenous catheter (Braun Medical; 20G x 1 in) was used to load the lumen with iohexol solution, careful not to disrupt atherosclerotic lesions, by slowly filling the lumen followed by full sample submersion in iohexol solution (5 mL) and allowed to stain via diffusion for 60 min. Each sample was then removed from iohexol and the lumen cleared of solution via absorption by placing non-woven surgical gauze on the vessel ends. Subsequently, micro-CT imaging of each specimen was performed as described above. Following micro-CT image acquisition, the sample was removed from the mounting apparatus and returned to 10% NBF for 24 hours, to allow contrast agent washout. Artery samples were then removed from 10% NBF, the lumen cleared of solution, and imaged by micro-CT again to confirm iohexol washout. Preliminary studies demonstrated 24 hours as a suitable time for sufficient destaining. After washout, samples were processed for conventional paraffin embedded histology.

Imaging data analysis.

Three-dimensional reconstruction of micro-CT data was performed using NSI efx-CT software (Rogers, Minnesota) and DICOM files were exported for further analyses. Data

analysis of the DICOM files, compiled for 3D visualization and interpretation, was performed using the open source software, 3D Slicer [27]. Three-dimensional visualization, cross sectional images, volume segmentation, and calcium metrics were generated using this software platform.

To demonstrate variable photon attenuation in adjacent soft tissues, line profiles were generated from micro-CT images across the artery wall before and after iohexol staining as well as with and without the presence of atherosclerotic plaques. Line profiles were generated from DICOM files using ImageJ [28]. The grey-value intensity along the length of the line profile was then plotted for representation.

Histological analysis.

Following micro-CT analysis of the entire artery length, vessel segments, 3-5 mm in length, were cut to fit into histology cassettes for standard processing. The samples were embedded in paraffin with the luminal axis perpendicular to the cutting face of the paraffin block. An additional micro-CT scan was performed, prior to sectioning, to accurately locate areas of interest in each sample cassette for comparison, due to tissue shrinkage during histological processing. This micro-CT scan was performed using the settings shown in the Table 1 of the supplementary materials, and the linear distance from the cutting edge of the paraffin block to the center of the calcium deposit was measured using 3D Slicer for each sample. This measurement was used as a reference for histology in order to accurately section each sample at the area of interest. Subsequently, specific segments identified by micro-CT imaging from each sample were sectioned for histology, based on representative calcium and plaque content of the artery overall.

Tissue specimens were conventionally processed for paraffin embedded histology and sectioned at 5 μm thickness using a HM355S motorized microtome (Thermo Scientific). Hematoxylin and eosin (H&E; tissue morphology) and Masson’s trichrome (fibrin and connective tissue) stainings were performed on serial sections from each region of interest. Slides were imaged using a Zeiss Axioplan2 microscope with a Zeiss 10x/0.45NA plan-apochromat objective and Zeiss AxioCam HRc digital camera.

Results

Individual line profiles.

Line profiles for control and iohexol stained samples were generated to demonstrate augmented radiopacity changes associated with iohexol contrast. Representative axial micro-CT cross-sections of coronary arteries without atherosclerotic plaques before (Fig. 1A) and after (Fig. 1B) iohexol staining demonstrate a marked change in radiopacity. Gray value intensities returned to control levels following iohexol washout in both control and atherosclerotic arteries (Fig. 1C and F, respectively). Similarly, atherosclerotic arteries revealed a notable change in radiopacity before diffusible contrast staining (Fig. 1D) and after staining (Fig. 1E). Of note, a focal, radio-dense region, representing calcium phosphate deposition, is identified within the atherosclerotic vessel (yellow circle).

Analysis of the gray values within the line profiles of these representative cross-sections revealed changes in radiopacity of an NBF fixed sample *vs.* the same sample that was subjected to radiopaque staining with iohexol (Fig. 1G and H). The shape of the profile was markedly changed after iohexol staining, increasing intensity at the adventitia followed by a constant grey value throughout the media in samples without plaques (Fig. 1E). A similar profile was observed in atherosclerotic arteries with an additional intensity peak through the lipid-rich atherosclerotic plaque. Interestingly, the large spike in intensity due to calcium phosphate deposition in the atherosclerotic vessel case (Fig. 1D) was attenuated by iohexol staining (Fig. 1E) but returned following iohexol washout (Fig. 1F). All gray values were normalized to the average plateau value of the sample without contrast, excluding the calcium peak in the atherosclerotic sample.

Contrast enhanced micro-CT.

Iohexol staining increased x-ray absorptivity in soft tissues, enhancing micro-CT image acquisition and subsequent image analysis. Vessels stained with iohexol demonstrated greater soft tissue delineation than unstained controls (Fig. 2). Without contrast agent, the soft tissue layers of the vessel wall and plaques were not discernable (Fig. 2A and C) and could not be separated into multiple segments (Fig. 2B and D). However, mineralized tissue such as calcium phosphate depositions, could be resolved using micro-CT without iohexol (Fig. 2C) and easily segmented (Fig. 2D). Staining with iohexol resulted in an enhanced micro-CT scan with delineated soft tissues comprising the vessel wall (Fig. 2E and G). Contrast-enhanced micro-CT allowed visualization of adventitia, smooth muscle, and endothelium as well as plaque size and morphology. These are represented by the colorized segmentation overlay of iohexol stained samples in Figures 2F and H.

Soft tissue segmentation in 3D space.

Micro-CT imaging provides 3D reconstruction of scanned samples allowing for improved analysis of physical structure and *in situ* architecture. Furthermore, micro-CT paired with diffusible contrast staining yields soft tissue delineation that can be visualized in 3D space (Fig. 3). Prior to iohexol staining, the soft tissues in the vessel walls were not discernable, generating an image with a solid, unresolved, segmentation (Fig. 3A and B). However, after staining with iohexol as a radiopaque contrast agent, connective tissue, smooth muscle, atherosclerotic plaque, and endothelium were resolved in the micro-CT image reconstruction and subsequently segmented (Fig. 3C–E). This enabled volumetric segmentation of micro-CT reconstructions of coronary arteries with atherosclerotic plaques, with cut away regions to show the topography and shape of the segmented layers with less cut away segmentations to better show plaque formation in the arterial wall (Fig. 3D and E). Furthermore, computed volumes for the individual segmentations can be generated using 3D slicer, providing analysis of atherosclerotic plaque development.

Calcium phosphate segmentation.

Calcium phosphate deposition was visualized in 3D space following reconstruction of micro-CT images and rapidly located within the atherosclerotic plaque using 3D Slicer (Fig. 4). Figure 4A shows full vessel reconstruction and volume segmentation while Figure 4B shows the same sample volume but with transparent soft tissue, illuminating the calcium

phosphate depositions (yellow) scattered throughout the atherosclerotic plaques that traverse the length of the artery. Figure 4C is a magnified image of the sample, showing the location of multiple calcium deposits in the wall of the artery. The lighter green shading along the vertical axis of the coronary artery in Figures 4B and C is representative of the vessel lumen. Some segments of the lumen are fully patent with other regions obstructed either by plaque or residual NBF.

Micro-CT and histology.

Micro-CT paired with iohexol as a radiopaque, diffusible contrast agent yields soft tissue delineation comparable to histological sectioning (Fig. 5). Segmentation of adventitia, smooth muscle, and plaque formation was compared to H&E and trichrome staining by visual assessment, demonstrating accurate volume segmentation using micro-CT imaging (Fig. 5A, D, and G). Micro-CT imaging also preserved *in situ* architecture to a greater degree compared to histology (Fig. 5B, E, and H) as histology processing and subsequent sectioning can be destructive to samples via dehydration and microtome sectioning (Fig. 5F and E, respectively). In addition, micro-CT without a contrast agent accurately located calcium deposits as confirmed by H&E staining (Fig. 5C and F).

Discussion

In the current study, we explored the use of micro-CT paired with an iodine-based radiopaque contrast agent for visualization and characterization of atherosclerotic lesions to determine the effectiveness of this method as an alternative to or complementary with routine histology. Our data demonstrate that micro-CT with contrast agent was able to discern atherosclerotic plaque distribution and provided tissue layer delineation but was incapable of distinguishing specific cellular components of the plaque. We also reveal that calcium phosphate deposition was readily visualized using micro-CT, independent of contrast agent.

Micro-CT has recently emerged as a non-destructive imaging modality, generating rapid 3D images allowing for full sample evaluation while maintaining sample integrity. Whole-specimen radiopaque staining has aimed to increase tissue contrast in specimens across numerous studies [12, 22, 24] allowing micro-CT to advance as a virtual histological method. Calcified coronary arteries imaged using micro-CT has been shown to generate high resolution full-volume data without radiopaque staining [29]. Similarly, the present study demonstrates a unique approach combining micro-CT with radiopaque staining to image and evaluate atherosclerotic plaques rapidly in coronary artery disease, *ex vivo,* while maintaining *in situ* architecture of vessel-plaque structure and allowing for subsequent histological analysis. Importantly, diffusible iohexol staining allowed tissue layer delineation, similar to findings by Panetta et al. (2015) but with augmented radiopacity, providing a strategy for imaging atherosclerotic samples with improved tissue delineation.

Many studies have demonstrated the capabilities of imaging soft tissues using micro-CT paired with contrast agents such as osmium, gold, and tungsten and without exogenous contrast [29] yielding a variety of segmentation capabilities. However, these heavy metal compounds are often toxic and require complex staining techniques. The lack of a contrast

agent limits radiographic results for analysis due to low inherent photon attenuation in soft tissues. The method developed for the current study offers a rapid, nontoxic approach for delineating soft tissues using micro-CT paired with iohexol, generating tissue segmentation complementary to histological analysis. This method is nondestructive in comparison to traditional histology processing. Conventional histological processing causes tissue shrinkage and requires destructive tissue sectioning by microtome [1], resulting in tissue artifact and even possible detachment of plaque from the arterial wall, potentially altering interpretation of plaque structure. Furthermore, micro-CT with radiopaque staining can be supplementary to subsequent histological analysis due to the lack of interference with routine histology staining. In effect, combining both strategies to provide rapid 3D visualization by micro-CT followed by in depth cellular analysis via histology is a unique approach for analyzing atherosclerotic plaque development, preserving data that may be lost to histological analysis alone, with better identification and localization of areas of interest for subsequent histological sectioning.

Although micro-CT is a relatively rapid and powerful imaging modality, it cannot match the cellular detail offered by histological evaluation. However, nano-computed tomography (nano-CT) is capable of providing even greater resolution with radiopaque staining than micro-CT, and potentially capable of discerning cellular components of the atherosclerotic plaques, including macrophage infiltration, collagen deposition, and fibrous cap formation [11]. Although, computed tomography machines are relatively expensive, the technology yields rapid imaging times (minutes to hours) compared to volumetric reconstruction of serially sectioned histology samples (days to weeks).

Micro-CT is susceptible to a unique set of artifacts such as sample shift and beam hardening that can degrade image quality [30]. Minimal sample shifting occurred in this study due to tissue shrinkage during micro-CT acquisition of the NBF fixed sample, in the presence and absence of iohexol, as the samples dehydrated slightly during the 50-minute scan. Sample shifting resulted in misaligned radiographs for 3D reconstruction and blurring of the reconstructed volume, a shortcoming that can be corrected in limited capacity by reconstruction software. To combat sample dehydration, solution (2-3 ml; NBF or iohexol) was loaded into the bottom of the conical vial during preliminary micro-CT scans, but this did not aid in offsetting tissue dehydration. Importantly, for this study, the NSI efX-CT reconstruction software (Rogers, Minnesota) corrected any shift resulting in radiograph realignment and improved image quality. Finally, beam hardening can occur due to photon scattering at high density material interfaces with high attenuation coefficients and was not present in this study.

Soft tissue segmentation by 3D analysis software of iohexol stained samples is subjective in nature. When comparing gray value intensities via line profiles across micro-CT cross-sectional images, the shape of the plots is reflective of relative tissue densities; however, background threshold and window selection of the CT data, in the processing software, for each scan, yields subjective plot magnitudes. It has been shown that the soft tissues that comprise the vessel wall can be delineated with radiopaque staining [31]. However, diffusible radiopaque staining, may generate a diffusion profile inherent to the ability of the contrast agent to traverse the tissue layers. This study indicated a partial diffusion profile in addition

to preferential accumulation of iohexol in lipid rich tissues. Longer staining times in iohexol solution may yield improved results, allowing for augmented perfusion of the tissue. However, if solely a diffusion profile were present, similar peak intensities would most likely be seen at the outer wall of the artery and inner lumen surface with decreasing intensity towards the center of the tissue. This was not observed in the absence or presence of atherosclerotic plaques. Using our novel approach, adventitia, media, atherosclerotic plaque, calcium phosphate, and endothelium were segmented based on differences of the intensity profiles generated by micro-CT data.

Taken together, the results of this study demonstrate micro-CT as a powerful imaging modality for evaluation of atherosclerotic plaque morphology in animal models *ex vivo* or post-mortem human samples, aiding characterization of plaque structure and assessing calcium deposition. Imaging soft tissues with micro-CT paired with a radiopaque contrast agent yields 3D analysis of atherosclerotic plaque morphology, maintaining sample integrity and *in situ* architecture and providing expedited evaluation procedures that may serve to complement conventional histological analysis.

Supplementary Material

Refer to Web version on PubMed Central for supplementary material.

Acknowledgments

The authors would like to thank Jeff Bray and Kalen Johnson for their technical expertise as well as the Image Analysis Laboratory at Texas A&M University for the use of their light microscopy imaging equipment.

Financial support

This study was supported by NIH R01 HL139903 (CLH), NIH K01 RR031274 (ANF), and NSF DGE:1746932 (AMGH).

References

[1]. Friedemann MC, Mehta NA, Jessen SL, et al., Introduction to Currently Applied Device Pathology, Toxicol Pathol, 2019;47:221–234. [PubMed: 30844339]

[2]. Gerneke DA, Sands GB, Ganesalingam R, et al., Surface imaging microscopy using an ultramiller for large volume 3D reconstruction of wax- and resin-embedded tissues, Microsc Res Tech, 2007;70:886–894. [PubMed: 17661361]

[3]. Geyer SH, Mohun TJ and Weninger WJ, Visualizing vertebrate embryos with episcopic 3D imaging techniques, ScientificWorldJournal, 2009;9:1423–1437. [PubMed: 20024516]

[4]. Mohun TJ and Weninger WJ, Imaging heart development using high-resolution episcopic microscopy, Curr Opin Genet Dev, 2011;21:573–578. [PubMed: 21893408]

[5]. Dauguet J, Peled S, Berezovskii V, et al., Comparison of fiber tracts derived from in-vivo DTI tractography with 3D histological neural tract tracer reconstruction on a macaque brain, Neuroimage, 2007;37:530–538. [PubMed: 17604650]

[6]. Landis EN and Keane DT, X-ray microtomography, Materials Characterization, 2010;61:1305–1316.

[7]. Senter-Zapata M, Patel K, Bautista PA, et al., The Role of Micro-CT in 3D Histology Imaging, Pathobiology, 2016;83:140–147. [PubMed: 27100885]

[8]. Mizutani R and Suzuki Y, X-ray microtomography in biology, Micron, 2012;43:104–115. [PubMed: 22036251]

[9]. Schambach SJ, Bag S, Schilling L, et al., Application of micro-CT in small animal imaging, Methods, 2010;50:2–13. [PubMed: 19706326]

[10]. Holdsworth D, Drangova M and Fenster A, A high-resolution XRII-based quantitative volume CT scanner, Medical Physics, 1993;20:449–462. [PubMed: 8497237]

[11]. Busse M, Muller M, Kimm MA, et al., Three-dimensional virtual histology enabled through cytoplasm-specific X-ray stain for microscopic and nanoscopic computed tomography, Proc Natl Acad Sci U S A, 2018;115:2293–2298. [PubMed: 29463748]

[12]. Metscher BD, MicroCT for comparative morphology: simple staining methods allow high-contrast 3D imaging of diverse non-mineralized animal tissues, BMC Physiol, 2009;9:11. [PubMed: 19545439]

[13]. Stephenson RS, Boyett MR, Hart G, et al., Contrast enhanced micro-computed tomography resolves the 3-dimensional morphology of the cardiac conduction system in mammalian hearts, PLoS One, 2012;7:e35299. [PubMed: 22509404]

[14]. Gignac PM and Kley NJ, Iodine-enhanced micro-CT imaging: methodological refinements for the study of the soft-tissue anatomy of post-embryonic vertebrates, J Exp Zool B Mol Dev Evol, 2014;322:166–176. [PubMed: 24482316]

[15]. Descamps E, Sochacka A, De Kegel B, et al., Soft tissue discrimination with contrast agents using micro-CT scanning, Belgian Journal of Zoology, 2014;144.

[16]. e Silva JMdS, Zanette I, Noël PB, et al., Three-dimensional non-destructive soft-tissue visualization with X-ray staining micro-tomography, Scientific reports, 2015;5:1–7.

[17]. Faraj KA, Cuijpers VM, Wismans RG, et al., Micro-computed tomographical imaging of soft biological materials using contrast techniques, Tissue Engineering Part C: Methods, 2009;15:493–499. [PubMed: 19485760]

[18]. Lusic H and Grinstaff MW, X-ray-computed tomography contrast agents, Chem Rev, 2013;113:1641–1666. [PubMed: 23210836]

[19]. Metscher BD, MicroCT for developmental biology: a versatile tool for high-contrast 3D imaging at histological resolutions, Dev Dyn, 2009;238:632–640. [PubMed: 19235724]

[20]. Jeffery NS, Stephenson RS, Gallagher JA, et al., Micro-computed tomography with iodine staining resolves the arrangement of muscle fibres, J Biomech, 2011;44:189–192. [PubMed: 20846653]

[21]. Li Z, Clarke JA, Ketcham RA, et al., An investigation of the efficacy and mechanism of contrast-enhanced X-ray computed tomography utilizing iodine for large specimens through experimental and simulation approaches, BMC Physiol, 2015;15:5. [PubMed: 26691327]

[22]. Gignac PM, Kley NJ, Clarke JA, et al., Diffusible iodine-based contrast-enhanced computed tomography (diceCT): an emerging tool for rapid, high-resolution, 3-D imaging of metazoan soft tissues, J Anat, 2016;228:889–909. [PubMed: 26970556]

[23]. Kuettner A, Trabold T, Schroeder S, et al., Noninvasive detection of coronary lesions using 16-detector multislice spiral computed tomography technology: initial clinical results, J Am Coll Cardiol, 2004;44:1230–1237. [PubMed: 15364324]

[24]. Wintermark M, Jawadi SS, Rapp JH, et al., High-resolution CT imaging of carotid artery atherosclerotic plaques, AJNR Am J Neuroradiol, 2008;29:875–882. [PubMed: 18272562]

[25]. Lillås BS, Tøndel C, Gjerde A, et al., Measurement of renal functional response using iohexol clearance—a study of different outpatient procedures, Clinical Kidney Journal, 2019:1–8.

[26]. Newell-Fugate AE, Lenz K, Skenandore C, et al., Effects of coconut oil on glycemia, inflammation, and urogenital microbial parameters in female Ossabaw mini-pigs, PloS one, 2017;12.

[27]. Fedorov A, Beichel R, Kalpathy-Cramer J, et al., 3D Slicer as an image computing platform for the Quantitative Imaging Network, Magnetic resonance imaging, 2012;30:1323–1341. [PubMed: 22770690]

[28]. Schneider CA, Rasband WS and Eliceiri KW, NIH Image to ImageJ: 25 years of image analysis, Nature methods, 2012;9:671–675. [PubMed: 22930834]

[29]. Panetta D, Pelosi G, Viglione F, et al., Quantitative micro-CT based coronary artery profiling using interactive local thresholding and cylindrical coordinates, Technology and Health Care, 2015;23:557–570. [PubMed: 26410117]

[30]. Boas FE and Fleischmann D, CT artifacts: causes and reduction techniques, Imaging in medicine, 2012;4:229–240.

[31]. Darrouzet S, MicroCT of Coronary Stents: Staining Techniques for 3-D Pathological Analysis, In, 2011.

Highlights:

- Iohexol contrast staining generated augmented three-dimensional segmentations of formalin-fixed coronary arteries due to increased radiopacity of the soft tissues
- Micro-CT imaging preserved atherosclerotic plaque morphology as compared to histologic analysis
- Our novel data reveal that micro-CT paired with iohexol is a powerful imaging modality that may serve to complement conventional histology procedures

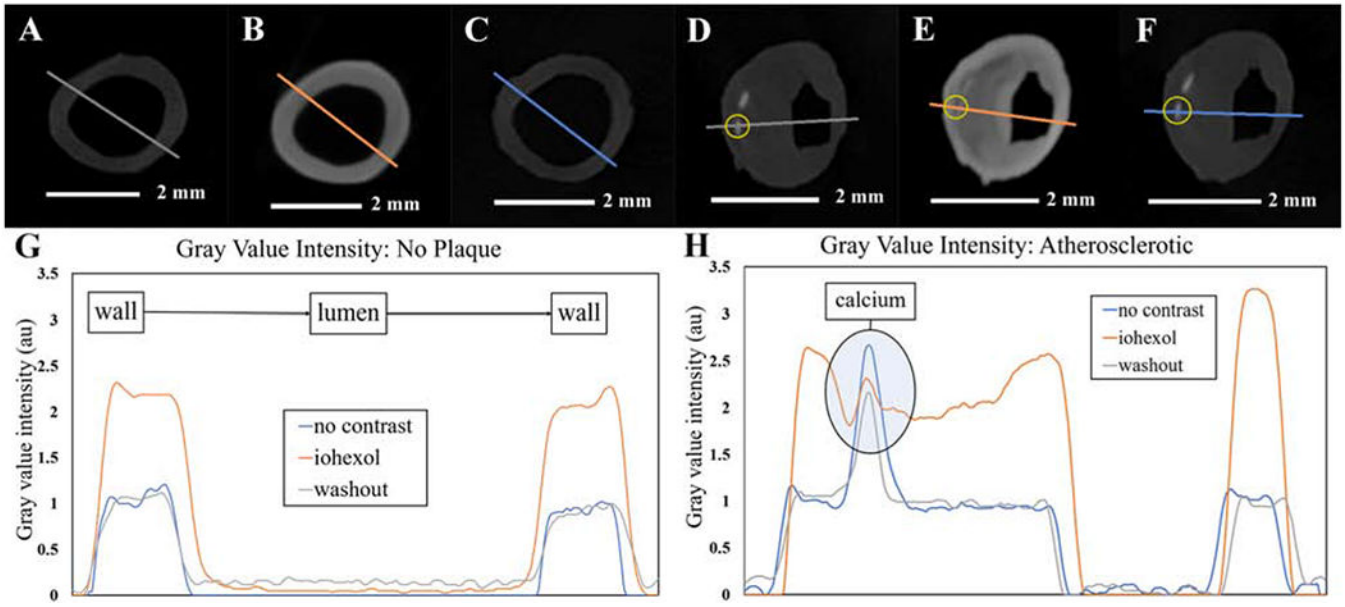

Figure 1:

Gray value intensities in the absence and presence of iohexol.

(A, B, and C) Micro-CT sections of the same control (no plaque) sample, with no contrast (A) following iohexol staining (B) and after iohexol washout (C) with the colorized lines representing the line profile paths. (G) Plotted gray value intensities along the paths in A, B, and C. (D, E, and F) Same micro-CT section of the same atherosclerotic sample with no contrast (D), following iohexol staining (E), and after iohexol washout (F), with colorized lines representing the line profile paths and the yellow circles indicating the location of calcium phosphate deposition. (H) Plotted gray value intensities along the paths in D, E, and F with noted calcium spikes.

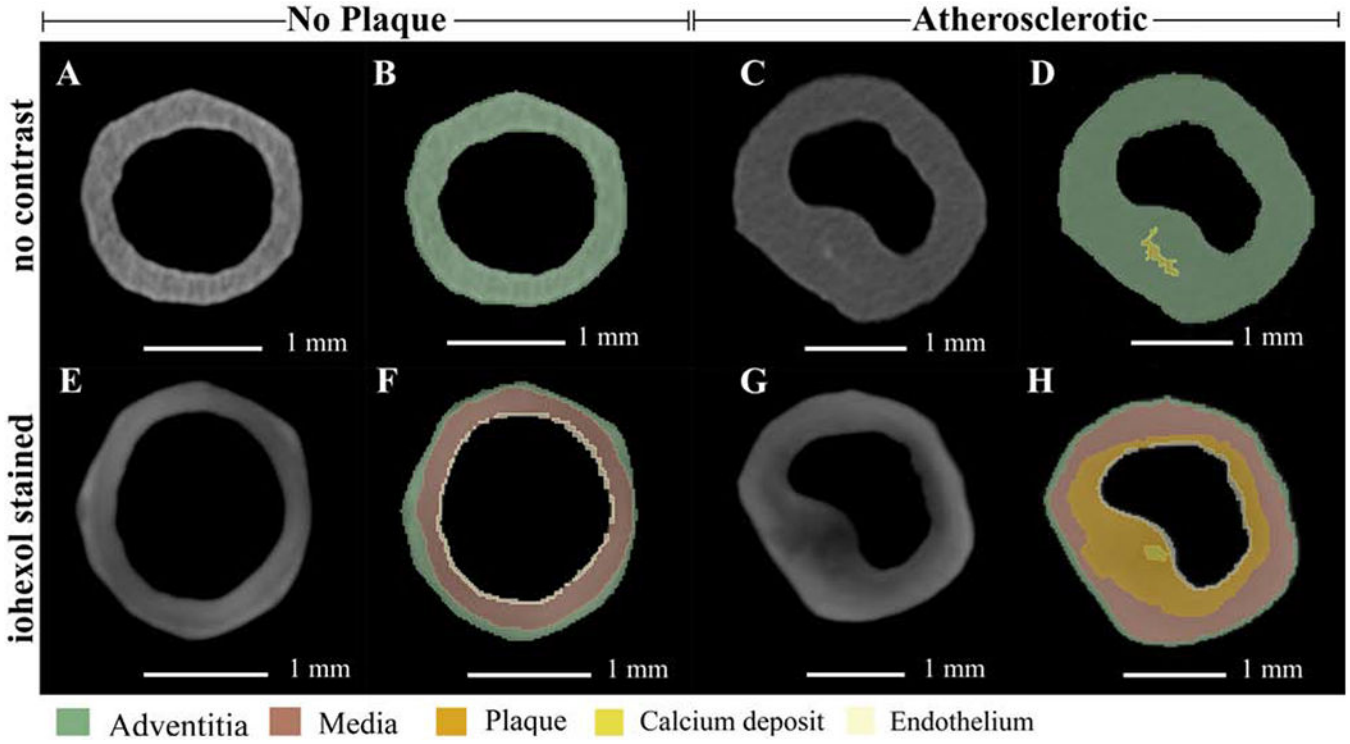

Figure 2:

Axial cross sections of micro-CT volumes in the absence and presence of iohexol with colorized overlays.

(A, B, E, and F) Micro-CT sections of the same control (no plaque) sample, at the same location, with no contrast (A and B) and with iohexol staining (E and F). Panels B and F are the colorized segmentation overlays of A and E respectively. (C, D, G, and H) Micro-CT sections of the same atherosclerotic sample, at the same location, with no contrast (C and D) and with iohexol staining (G and H). Panels D and H are the colorized segmentation overlays of C and G, respectively. With no contrast agent, segmentation was limited. Iohexol staining augmented the segmentation capabilities of micro-CT images with volumes generated for adventitia, media, plaque, calcium, and endothelium.

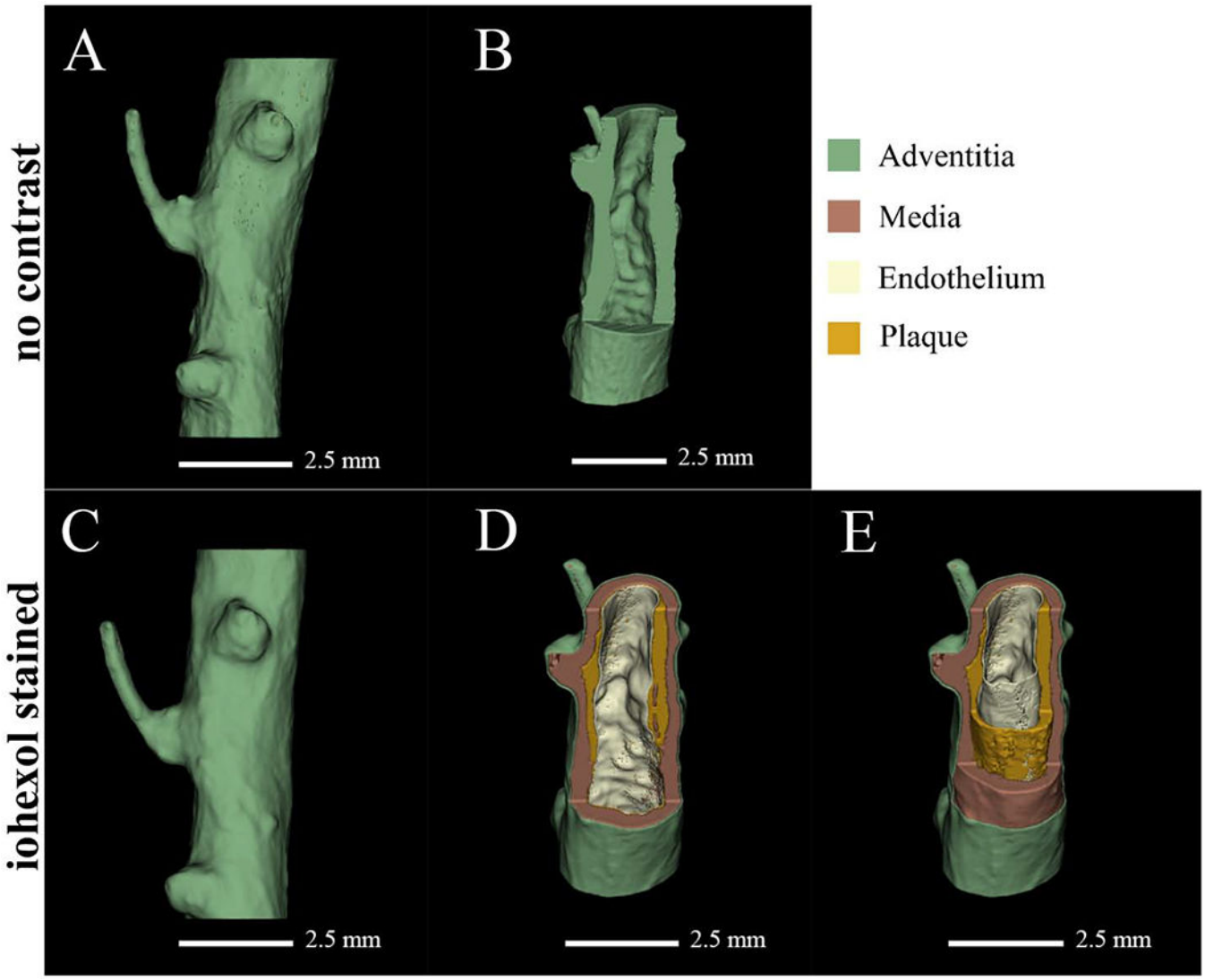

Figure 3:

Full volume reconstruction and visualization of a coronary artery in the absence and presence of iohexol.

The same sample is illustrated in panels A-E with no contrast (A and B) and iohexol staining (C-E). Panels A and C show full volume reconstructions while panels B, D, and E have cut away sections to illuminate detail. Iohexol staining (C-E) aided higher resolution segmentation, as shown in panels D and E; resolving adventitia, media, plaque, and endothelium.

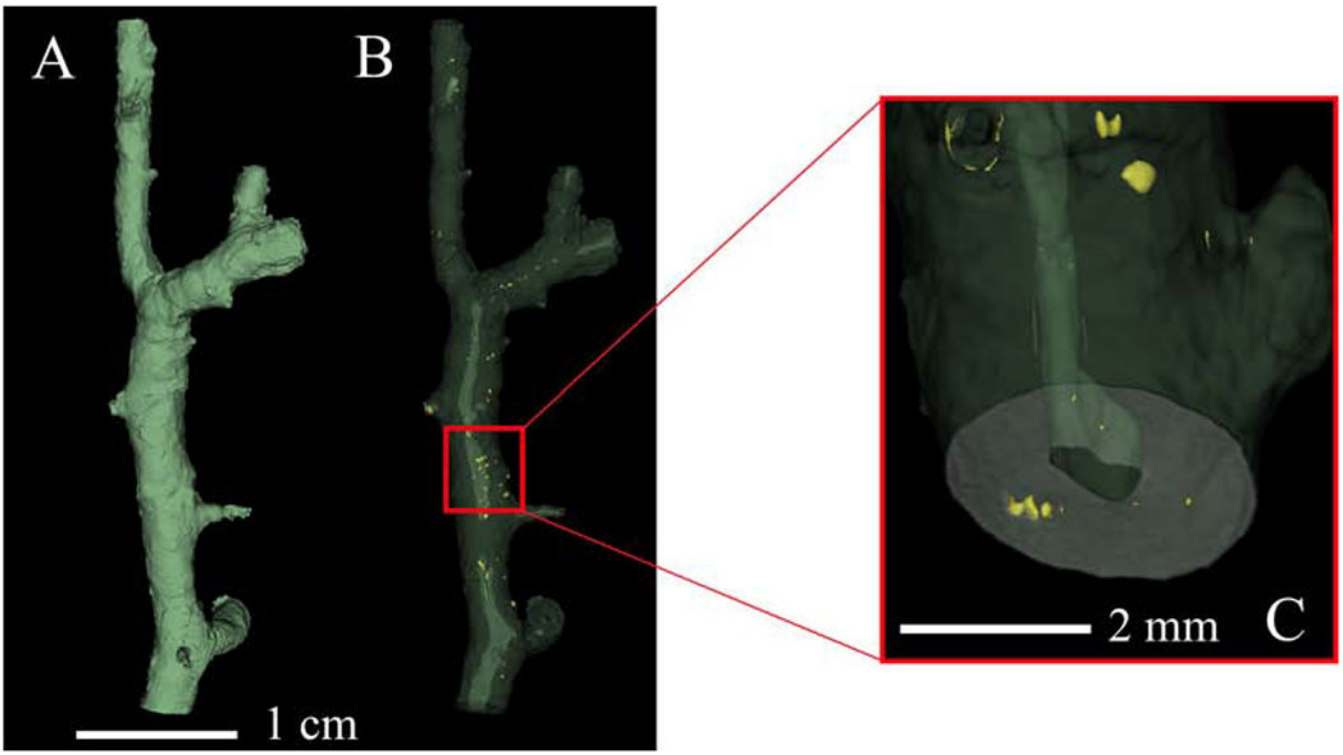

Figure 4:

3D visualization of calcium phosphate deposition. Calcium phosphate is segmented without the aid of a contrast agent.

(A) Full volumetric reconstruction of the micro-CT scanned sample. (B) Same volume represented in panel A but with phased out soft tissue (green) and with segmented calcium phosphate (yellow). (C) Magnification of a section in panel B illuminating calcium phosphate deposition (yellow) in the artery wall.

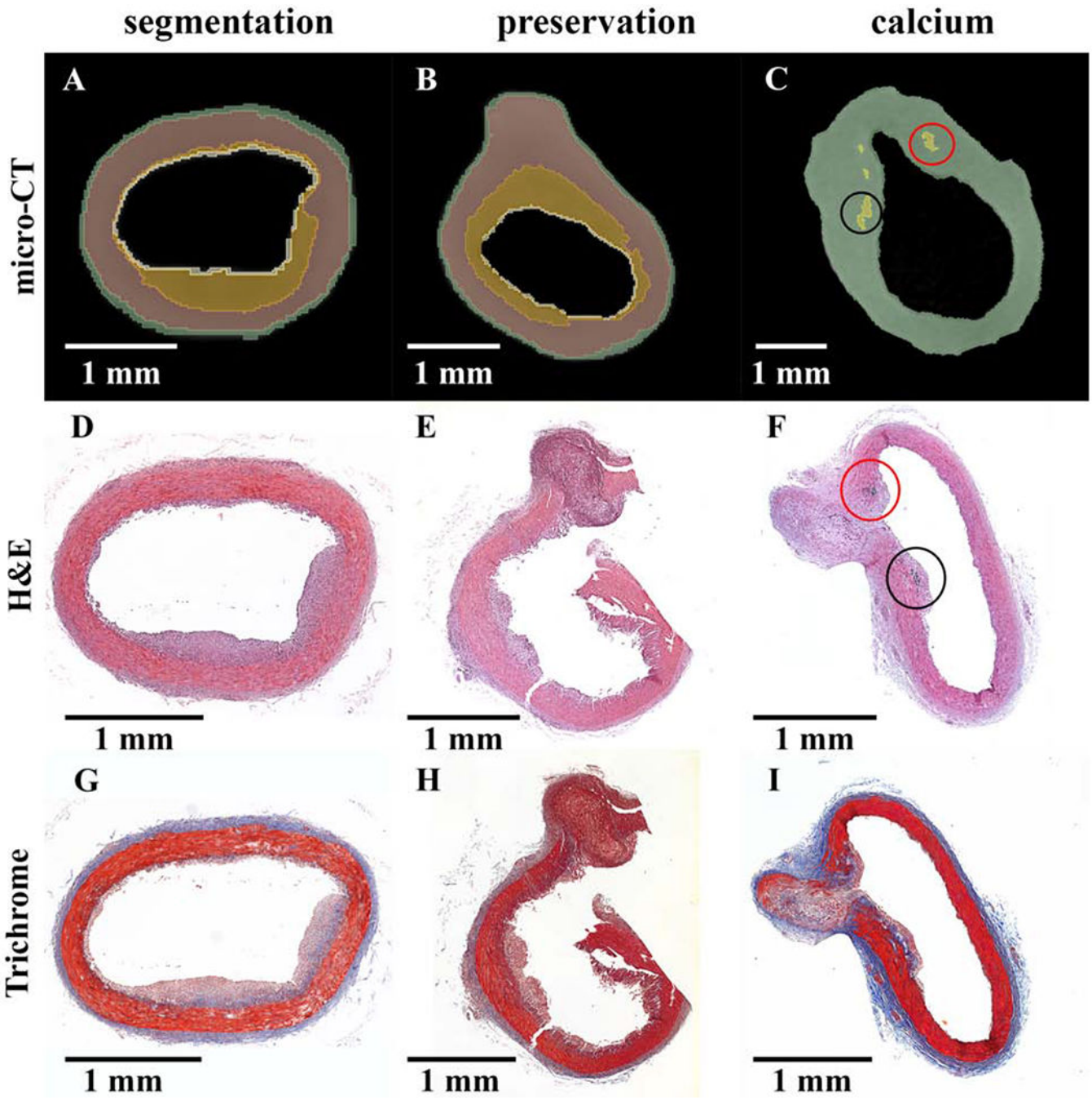

Figure 5:

Preservation of in situ architecture: micro-CT and histology comparison.

(A-C) Micro-CT sectioning with colorized overlay. (D-I) Histology sections stained with H&E (D-F) and Masson's trichrome (G-I). Each column is a single sample with the micro-CT image matched to the relative H&E slide. Column 1 (segmentation) illustrates the micro-CT segmenting capabilities of iohexol stained atherosclerotic vessels. Column 2 (preservation) shows the preservation of sample integrity by micro-CT with contrast agent, whereas tissue damage may occur with histology sectioning. Column 3 (calcium) indicates

calcium segmentation by micro-CT without contrast matched to positive H&E staining of calcium phosphate at the base of the plaque structure. Both columns 2 and 3 reflect vessel structure at the site of an arterial branch point.